ARTICLE
Journal of Cellular Biochemistry 107:418–427 (2009)

Journal of Cellular Biochemistry

Control Mechanisms of Differential Translation of Hsp90 Isoforms in 9L Rat Gliosarcoma Cells

Chih-Wei Lo,[1] Yuo-Sheng Chang,[1] Chih-Chung Chao,[1] Margaret Dah-Tsyr Chang,[2] Kun-Che Chang,[1] and Yiu-Kay Lai[1,3*]

[1]*Department of Life Science, Institute of Biotechnology, National Tsing Hua University, Hsinchu 30013, Taiwan, ROC*

[2]*Department of Life Science, Institute of Molecular and Cellular Biology, National Tsing Hua University, Hsinchu 30013, Taiwan, ROC*

[3]*Department of Bioresources, Da-Yeh University, Changhua 51591, Taiwan, ROC*

ABSTRACT

Although the differential expression of heat shcok proteins, Hsp90α and Hsp90β was extensively studied in many kinds of cells, the post-transcriptional regulation of Hsp90 isoforms remains unclear. In control and GA-treated rat gliosarcoma cells, it has been reported that the translational efficiency of *hsp90α* is higher than *hsp90β*. In this study, we present evidences identifying the roles for leaky scanning and 5′-UTR sequence in translational regulation of Hsp90β. The result of in vitro transcription and translation (IVTT) experiment showed that *hsp90α* exhibited higher translation efficiency than *hsp90β*. Sequence analysis revealed that there is an out-of-frame downstream AUG codon in *hsp90β* gene. However, elimination of the downstream AUG by site-directly mutagenesis or introducing Kozak context sequence around the initiator AUG of *hsp90β* open reading frame increased its translational efficiency, which indicated that leaky scanning might be a possible mechanism regulating *hsp90β*. Furthermore, we also constructed a firefly luciferase reporter system to verify the effect of subsequent translation at the downstream out-of-frame AUG codon in 9L and A549 cells. Furthermore, it is believed that 5′-untranslated region (5′-UTR) also plays a significant role in translational control. We showed *hsp90β* 5′-UTR gives rise to the reduction of the translation efficiency in IVTT experiment. Additionally, the reductive effect of *hsp90β* 5′-UTR was further confirmed by luciferase reporter assay using truncated deletion analyses of 5′-UTR of *hsp90β*. Our results support the hypothesis that ribosome leaky scanning mechanism and 5′-UTR sequence acts as negative regulators in *hsp90β* mRNA. J. Cell. Biochem. 107: 418–427, 2009.

KEY WORDS: HEAT SHOCK PROTEIN 90; POST-TRANSCRIPTIONAL CONTROL; TRANSLATION EFFICIENCY; LEAKY SCANNING; 5′-UNTRANSLATED REGION

Heat shock proteins (Hsps) belong to the stress protein superfamily, serve as molecular chaperones and play critical roles in protein folding, signal transduction, and proteasome mediated protein degradation [Neckers and Ivy, 2003; Wegele et al., 2004; Liu et al., 2007]. Hsp90, the 90 kDa molecular chaperone comprising 1–2% of cellular proteins under non-stress conditions is one of the most abundant proteins in eukaryotic cells and the major core of a so-called cytosolic molecular chaperone complex [Pearl and Prodromou, 2001; Picard, 2002]. Exposure of Hsp90 inhibitors such as geldanamycin (GA), radicicol, or their analogs generally leads to rapid release of bound client proteins and disrupts the chaperone complex [Pratt and Toft, 2003].

Hsp90 is highly conserved from prokaryotes to eukaryotes. In mammalian cells, two functionally similar Hsp90 isoforms, known as Hsp90α and Hsp90β in human (Hsp86 and Hsp84 in mouse), have been identified [Csermely et al., 1998; Picard, 2002]. These two isoforms are generally around 85% identical in amino acid sequences but encoded by separate genes [Moore et al., 1989; Chen et al., 2005]. However, the nucleotide sequences of *hsp90α* and *hsp90β* have much less similarity as compared to their translated amino acid sequences, particularly in their 5′- and 3′-untranslated regions (5′-UTR and 3′-UTR), the introns, and the 5′-flanking sequences [Hickey et al., 1989; Gupta, 1995]. Unlike most eukaryotic genes encoding Hsps, *hsp90α* and *hsp90β* are composed of several

Grant sponsor: VGHUST; Grant numbers: 96-G2-02-5, 97-G2-4; Grant sponsor: NSC; Grant number: 97-3112-B-007-006.

*Correspondence to: Dr. Yiu-Kay Lai, Department of Bioresources, Da-Yeh University, Changhua 51591, Taiwan, ROC. E-mail: lslyk@life.nthu.edu.tw

Received 2 January 2009; Accepted 17 February 2009 • DOI 10.1002/jcb.22138 • 2009 Wiley-Liss, Inc.
Published online 23 March 2009 in Wiley InterScience (www.interscience.wiley.com).

introns and exons [Sreedhar et al., 2004]. In human *hsp90* genes, introns containing several heat shock elements (HSEs) have been reported to be associated with the inducible *hsp90α* gene expression and highly constitutive expression of *hsp90β* [Shen et al., 1997; Zhang et al., 1999]. Several studies also evaluated the regulation of *hsp90* genes at both transcriptional and translational levels [Hansen et al., 1991; Jacquier-Sarlin et al., 1995; Ahmed and Duncan, 2004; Chao et al., 2008]. But the features of the molecular mechanisms remained to be unraveled.

In general, Hsp90β is expressed constitutively to a higher level than Hsp90α in most mammalian cells, and is involved in long-term cellular adaptation. In some cases, Hsp90β was highly expressed in chronic tumors [Ogata et al., 2000], the development of multi-drug resistance [Bertram et al., 1996] and maintenance of the cytoarchitecture [Sreedhar et al., 2003]. In contrast, *hsp90α* is highly inducible under stress and may therefore be important for cytoprotection, such as its selective induction in nicotine-induced apoptosis [Wu et al., 2002]. Hsp90α is also expressed to high-level in acute cancers, such as breast cancer [Jameel et al., 1992] and pancreatic carcinoma [Gress et al., 1994]. In addition, the high expression of *hsp90α* was considered to be correlated to tumor progression [Yufu et al., 1992] and enhanced cell cycle regulation [Jerome et al., 1993]. Thus, a differential induction/expression manner between Hsp90 isoforms exists in response to various extracellular signals and stress. In our previous study, it was found that rat *hsp90α* and *hsp90β* translated at different rates [Chang et al., 2006]. The crucial role of such differential translation efficiency and the underlying molecular mechanism remained unclear.

Translational control is a final step in a complex network of regulatory processes involved in the control of gene expression [Kozak, 2007]. In most eukaryotes, translation initiates predominantly by a ribosome scanning mechanism [Kozak, 1999, 2002a,b], and that a scanning ribosome chooses an AUG codon to serve as a translation initiation site is modulated by some parameters. The context of nucleotides flanking an AUG codon contributes largely to the efficiency of translation initiation. The reputed Kozak consensus sequence, having the optimal context of GCC**R**CCAUG**G**, offers the greatest enhancement on translation initiation [Kozak, 1999]. The most important positions for efficient translation are a purine at position −3 and a G nucleotide followed by AUG at position +4 [Kozak, 1986]. Suboptimal recognition of an initiator codon results in a portion of ribosome complex continuing to scan and initiating at a downstream site, in a process known as leaky scanning [Kozak, 1989], for example, in the tricistronic S1 mRNA of avian reovirus [Racine et al., 2007]. In addition to leaky scanning, three additional mechanisms of less commonly used alternative translation initiation including ribosome re-initiation, shunting, and internal ribosome binding have been described [Jackson, 2005].

Sequence and structural elements encircled within the 5′-UTR of mRNAs are also believed to play a significant role in translational control. These elements regulate translation efficiency and stability of mRNAs by acting as binding sites for *trans*-acting factors [McCarthy and Kollmus, 1995]. Most *hsp* 5′-UTRs are long (150–250 nucleotides) and rich in A residues (∼50%), which reduces secondary structure [Lindquist and Petersen, 1990]. Nevertheless, the investigation of the 5′-UTR sequences of *hsp90* isoform mRNAs revealed several elements with the potential to form a stable secondary structure, which in turn might mediate translational control of mRNAs of *hsp90* isoforms. The 5′-UTR sequences of rat *hsp90α* and *hsp90β* mRNA are 57 and 85 nucleotides in length, respectively. The GC content is higher in *hsp90β* (64.7%) than that of *hsp90α* (57.1%). GC-rich regions are known to have a high potential to form stable secondary structures [Kozak, 1991b], which results in inability of the ribosomal complex to unwind the secondary structure and reach the AUG codon [Kozak, 1991a,b], and finally confers the regulation of translation.

In this study, we employed in vitro transcription and translation (IVTT) systems and luciferase reporter system to investigate the mechanisms involved in differential translation efficiency of rat Hsp90 isoforms. We also identified and characterized the leaky scanning mechanism for translation regulation of *hsp90β* mRNA. Furthermore, we also discovered that the secondary structure at 5′-UTR indeed involved in the regulation of translational efficiency of *hsp90β* mRNA. These results suggest that the leaky scanning and the 5′-UTR sequences serve as negative regulatory elements for translation efficiency of Hsp90β.

MATERIALS AND METHODS

MATERIALS

Geldanamycin (GA) was purchased from Sigma Chemicals and dissolved in dimethyl sulfoxide (DMSO) at a stock concentration of 1 mM and stored in dark at −20°C. *Pfu* DNA polymerase (Promega) was used to amplify all the PCR products. Synthetic oligonucleotides were ordered from MISSION BIOTECH. [^{35}S]methionine (specific activity >800 Ci/mmol) was purchased from Amersham Biosciences. Restriction enzymes used for cloning and modifying DNA were purchased from New England Biolabs.

CELL CULTURE AND DRUG TREATMENTS

Rat gliosarcoma 9L cell line [Weizsaecker et al., 1981] was cultured in Eagle's minimum essential medium with Earle's salts (MEM, Invitrogen); human lung cancer cell line A549 was maintained in Dulbecco's modified Eagle's medium (DMEM, Invitrogen). All of the culture media were supplemented with 10% fetal bovine serum (HyClone), 100 U/ml penicillin G, and 100 μg/ml streptomycin (Sigma), at 37°C under a 5% CO_2 atmosphere. Exponentially growing cells at 70–80% confluence were used, maintained, prior to each experiment, and stock cells were plated in 25 cm^2 flasks or 6-well plates at a density of 4–6 × 10^4 cells/cm^2. The cells were treated with 0.5 μM GA for 6 h for protein analysis or 5 h for preparation of RNA.

DE NOVO SYNTHESIS

At the end of GA treatment, cells were metabolically labeled with [^{35}S]methionine at a concentration of 20 μCi/ml for 1 h before harvested. The cells were briefly rinsed in phosphate-buffered saline (PBS) and lysed with sample buffer [Laemmli, 1970] as previously described [Lee et al., 1993]. The cell lysates were then resolved by 7.5% SDS–PAGE (pH 8.0) and processed for autoradiography.

Protein bands of interest in the autoradiograms were quantified by densitometric scanning (Molecular Dynamics).

RNA ISOLATION AND NORTHERN BLOT ANALYSIS

Total cellular RNA was extracted from approximately 1×10^6 cells using Trizol reagent (Invitrogen) according to the manufacturer's specifications. Northern blot analysis and digoxigenin (DIG)-labeled probes were carried out as described [Chang et al., 2006].

IN VITRO TRANSCRIPTION AND TRANSLATION (IVTT)

Coupled transcription–translation (system programmed with plasmid DNA) of the construct plasmid DNA, under the control of the T7 RNA polymerase promoter, was carried out by using the $T_NT^{®}$ Quick Coupled transcription–translation system according to the manufacturer's instructions (Promega), containing [^{35}S]methionine at a concentration of 20 μCi/ml. Standard reactions were performed essentially as recommended by the manufacturer in a total reaction volume of 25 μl. Incubation was for 90 min at 30°C. Equal amounts (5 μl aliquot) of the reaction products were resolved by 10% SDS–PAGE gel. After electrophoresis, the gels were fixed, dried and processed for autoradiography by using FuJi FILM RX X-ray film. Protein bands of interest in the autoradiograms were quantified by densitometric scanning.

CONSTRUCTION OF THE IVTT ASSAY PLASMIDS

The full-length of rat *hsp90α* and *hsp90β* genes, including 5′-UTR, coding sequence (CDS) and 3′-UTR, were constructed into the pET21(+) plasmid (Novagen) with T7 promoter. The rat *hsp90α* and *hsp90β* genes were amplified from cDNA product of the rat 9L cells by using *pfu* DNA polymerase (Promega). The construct of full-length *hsp90α* (pET-*hsp90α*) was prepared using following PCR primer combinations: rhsp90α-1, spanning from 1 to 611 nucleotide (rhsp90α1-forward, 5′-GTTGCTTCAGTGTCCCGGTG-3′ and rhsp90α1-reverse, 5′-TTTGTTCCACGACCCATTGG-3′); rhsp90α-2, 521–1922 nucleotide (rhsp90α2-forward, 5′-TGATGACGAGCAGTACGCC-3′ and rhsp90α2-reverse, 5′-TTGTCTCTGAGGGCTTGAGC-3′); rhsp90α-3, 1825–2781 nucleotide (rhsp90α3-forward, 5′-ACCGATTGGTGACATCC-3′ and rhsp90α3-reverse, 5′-TGCGGCCGCTTTTTATCTCATCTGTATTTACC-3′) (*Not*I restriction site is underlined). The three amplified fragments were digested with *Bam*HI, *Bam*HI/*Nde*I, and *Nde*I/*Not*I, respectively. For construction of the full-length *hsp90β* (pET-*hsp90β*), the followed another PCR primer combinations were used: rhsp90β-1, spanning from 1 to 1568 nucleotide (rhsp90β1 forward, 5′-CCCGCGCAGCCTAGGC-3′ and rhsp90β1 reverse, 5′-CACCTGCTCTTTGCTCTCACC-3′); rhsp90β-2, 1327–2511 nucleotide (rhsp90β2 forward, 5′-GCTCTTCTCTGAGTTGGC-3′ and rhsp90β2 reverse, 5′-TGCGGCCGCTATAAAACTGCATCATCTTTATTTTGC-3′) (*Not*I restriction site is underlined). The two amplified fragments were digested with *Hin*dIII and *Hin*dIII/*Not*I, respectively. The target pET21(+) vector was generated by digesting with *Bam*HI, blunting with DNA polymerase (Klenow, Promega), then digesting with *Not*I. All PCR-amplified fragments were purified after gel electrophoresis using a Gel/PCR DNA Fragments Extraction kit (Geneaid), and then inserted into digested pET21(+) vector using their respective restriction sites.

Plasmid pET-*hsp90β*m1 and pET-*hsp90β*m2 were introduced using pET-*hsp90β* as a template and the QuickChange® site-directed mutagenesis kit (Stratagene) as recommended by the manufacturer. The following primers were used: rhsp90βm1-forward, 5′-GCACCAAGGAGAGGAAGAGG-3′ and rhsp90βm1-reverse, 5′-CCTCTTCCTCTCCTTGGTGC-3′ (mutated AUG is underlined) for pET-*hsp90β*m1; rhsp90βm2-forward, 5′-CTCGGCTTTCTCGCCACCATGGCTGAGGAAGTGCACC-3′ and rhsp90βm2-reverse, 5′-GGTGCACTTCCTCAGCCATGGTGGCGAGAAAGCCGAG-3′ for pET-*hsp90β*m2. The introduced mutation was verified by DNA sequencing.

Plasmid pET-*βhsp90α* and pET-*αhsp90β* were obtained by the replacement of a region to generate the 5′-UTR exchange constructs. The rhsp90β1-forward primer and rhsp90αex-reverse primer, 5′-CTGCCTGAAAGGCAAAGG-3′ were used to amplify the following synthetic nucleotides encoding partial *hsp90α* gene with *hsp90β* 5′-UTR sequence: CCCGCGCAGCCTAGGCTTGCCGTGCGAGTCGGACGTGGTCCGGGCCCACCCTGCTCTGTACTACTACTCGGCTTTCTCGTCAAGATGCCTGAGGAAACCCAGACCCAAGACCAACCAATGGAGGAAGAGGAGGTCGAAACCTTTGCCTTTCAGGCAG (the start codon of *hsp90α* was underlined). In addition, the rhsp90α1-forward primer and rhsp90βex-reverse primer, 5′-GTGTTGATGATGAGGGACATCA-3′ were used for the following synthetic nucleotides encoding partial *hsp90β* gene with *hsp90α* 5′-UTR sequence: GTTGC TTCAGTGTCCCGGTGCGGTTAGTCACGTTTCGTGCGTGCTCATTCTGCCAAGATGCCTGAGGAAGTGCACCATGGAGAGGAAGAGGTGGAGACCTTCGCCTTTCAGGCAGAAATTGCCCAGCTGATGTCCCTCATCATCAACAC (the start codon of *hsp90β* was underlined). The rhsp90αex-forward primer, 5′-AAATTGCCCAGTTAATGTCC-3′ and rhsp90βex-forward primer, 5′-TTTCTACTCAAACAAAGAGATTTTCC-3′ were paired with the rhsp90ex-reverse primer, 5′-TCCTAGAGGGGAATTGTTATCCGC-3′ to produce the rest of pET-*hsp90α* and pET-*hsp90β*, respectively. Then, they were blunt-end ligated to generate the pET-*βhsp90α* and pET-*αhsp90β* constructs.

PLASMID TRANSFECTION AND LUCIFERASE REPORTER ASSAY

For transient transfection, 9L cells were seeded at 5×10^5 in a 12-well plate for 1 day prior to transfection (90–95% cell confluence). Cells were transfected with equal amount of the individual reporter plasmids using LipofectAMINE™ 2000 reagent (Invitrogen) following the manufacturers' instruction. The pRL-CMV vector (Promega), containing the CMV enhancer and early promoter elements to provide high-level expression of *Renilla* luciferase, were co-transfected as an internal control. After 48 h transfection, the cells were washed twice with PBS and lysed by passive lysis buffer (Promega). The lysates were centrifuged at 11,000*g* for 1 min at 4°C, and the supernatant was collected. The firefly and *Renilla* luciferase activities were measured by TD-20/20 luminometer (Victor), and the luciferase results were reported as relative light units of firefly luciferase activity normalized with respect to the *Renilla* luciferase activity. Error bars represent the standard errors for at least three independent experiments.

CONSTRUCTION OF THE LUCIFERASE REPORTER PLASMIDS

The 5′-UTR and 3′-UTR sequence of *hsp90α* and *hsp90β* were obtained by PCR synthesis from the rat 9L cDNA. They were inserted

into the pGL3 promoter vector (pGL3p, Promega), which contained the simian virus (SV40) promoter and firefly luciferase gene and from which the SV40 late poly(A) signal had been excised. The pGL3 basic vector (pGL3b, Promega), has no SV40 promoter and enhancer, was used for the promoterless assay. The 5′-UTRs were inserted between the *Hin*dIII and *Nco*I sites. And the 3′-UTRs were cloned into the *Xba*I site then the orientation of insertion sequences were determined by DNA sequencing.

The primer sequence of the 5′-UTRs for *hsp90α* 5′-UTR: *Hin*dIII-α5′ forward primer, 5′-ATTAAGCTTGTTGCTTCAGTGTCCCGGTGC-3′ and *Nco*I-α5′ reverse primer, 5′-AACCATGGCTTGGCAGAAT-GAGCACGCACG-3′. The primers used for *hsp90β* 5′-UTR: *Hin*dIII-β5′ forward primer, 5′-ATTAAGCTTCCCGCGCAGCCTAGGCTTGC-3′ and *Nco*I-β5′ reverse primer, 5′-AACCATGGCTTGACGAGAA-AGCCGAGTAG-3′. The primer sequence of the 3′-UTRs for *hsp90α* 3′-UTR: *Xba*I-α3′ forward primer, 5′-TTCTAGAGCTTCACCAGAAC-TATGTGTTTGATGC-3′ and *Xba*I-α3′ reverse primer, 5′-TTCTA-GATTTTTATCTCATCTGTATTTACC-3′. The primers used for *hsp90β* 3′-UTR: *Xba*I-β3′ forward primer, 5′-TTCTAGAAGGCTCCTGG-GAAGCCCCCGCC-3′ and *Xba*I-β3′ reverse primer, 5′-TTCTAGA-TATAAAACTGCATCATCTTTATTTTGC-3′. The PCR products of *hsp90* isoforms 5′-UTRs and 3′-UTRs were digested and purified after gel electrophoresis, and then ligated into pGL3p and pGL3b vectors, which had been digested with respective restriction sites.

REVERSE-TRANSCRIPTASE POLYMERASE CHAIN REACTION (RT-PCR)

Reverse transcription was performed on each RNA sample (0.5 μg) using oligo-dT and M-MLV reverse transcriptase (Promega). Primers specific for firefly luciferase, spanning in 148 bps (rFFL-forward, 5′-GCCCGCGAACGACATTTA-3′ and rFFL-reverse, 5′-TTTGCAACCC-CTTTTTGGAA-3′), and *Renilla* luciferase, spanning in 148 bps (rRL-forward, 5′-GCAGCATATCTTGAACCATTCAAA-3′ and rRL-reverse, 5′-CATCACTTGCACGTAGATAAGCATTATA-3′), were designed to determine the mRNA amounts of the transient transfection plasmids. The endogenous actin gene (ractin-forward, 5′-AGGCCAACCGT-GAAAAGATG-3′ and ractin-reverse, 5′-CAGTGGTACGACCAGA-GGCATA-3′) was used as an internal standard to normalize the amount of total RNA present in each reaction. The above three respective pairs of primers were also used in real-time qPCR experiments. Each PCR product was electrophoresed on 2% agarose gels.

REAL-TIME QUANTITATIVE PCR (REAL-TIME QPCR)

The mRNA levels of firefly and *Renilla* luciferase were measured by SYBR GREEN PCR Master Mix and quantified using an ABI PRISM 7500 sequence detector system (Applied Biosystems). Real-time qPCR was performed in triplicate reactions with 4 ng cDNA in a final volume of 10 μl containing 1× SYBR Green PCR Master Mix (Applied Biosystems) and 0.1 μl of the above three respective pairs of primers. Samples were pre-heated at 95°C for 10 min and performed for 40 cycles (94°C for 15 s and 60°C for 1 min) of amplification. The endogenous actin gene were used to normalize the amount of total RNA present in each reaction and the comparative ΔC_t (threshold cycle number) ($\Delta\Delta C_t$) method were calculated to compare the expression levels among different samples [Livak and Schmittgen, 2001].

RESULTS

DIFFERENTIAL TRANSLATION EFFICIENCY OF hsp90 ISOFORM MRNAS

Hsp90-specific inhibitor, GA, has been used as an effective inducer of many stress proteins in previous reports [Lai et al., 2003; Shu et al., 2005; Chang et al., 2006; Chao et al., 2008]. In this study, the nascent proteins and mRNAs of Hsp90 isoforms (Hsp90α and Hsp90β) in the absence and presence of 0.5 μM GA treatment were respectively determined using de novo protein synthesis and Northern blot analysis as previously described [Chang et al., 2006]. The results of metabolic labeling showed that maximal expression levels of nascent Hsp90α and Hsp90β were induced by GA for 6 h when comparing with control levels (Fig. 1A). In addition, Northern blot analysis revealed that the transcripts of both genes were significantly increased upon treatment with GA for 5 h (Fig. 1B), and the absolute mRNA amount of *hsp90β* was significantly higher than that of *hsp90α* at both basal and inductive levels.

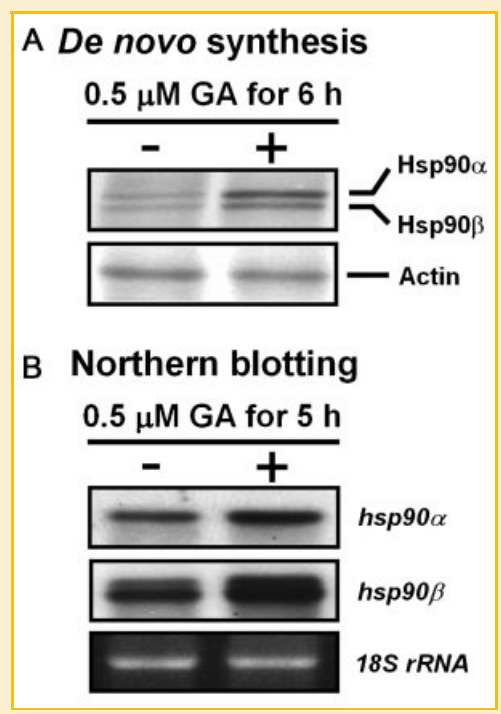

Fig. 1. Effects of GA on protein synthesis and mRNA abundance of Hsp90. Cells were treated with 0.5 μM GA for the indicated time duration. A: For de novo protein synthesis, cells were labeled with [^{35}S]methionine for 1 h before harvested. Equal amount of labeled cell lysates was resolved by 9% SDS–PAGE (pH 8.0) and processed for autoradiography. Bands of Hsp90α and Hsp90β in autoradiograph were showed. The bands of actin divided in the same lane were used as loading control. B: Northern blot analysis of total RNA (5 μg) from cells treated with DMSO or 0.5 μM GA for 5 h was carried out with the DIG-labeled *hsp90α*- and *hsp90β*-specific probe, respectively. The amount of 18S rRNA was used as a reference control.

It was particularly noteworthy that although slightly more nascent proteins of Hsp90α was induced by GA treatment, the mRNA level of *hsp90β* was significantly higher than that of *hsp90α*. In our previous study, the disproportion was correlated with differential translation efficiency (i.e., protein synthesis per mRNA), for the translation of *hsp90α* mRNA was significantly more effective than that of *hsp90β* under normal and GA-treated conditions [Chang et al., 2006]. Herein, a series of experiments were designed to clarify the mechanisms involved in the regulation of translation efficiency.

EFFECT OF LEAKY SCANNING ON THE TRANSLATION EFFICIENCY OF *hsp90β*

Sequence analysis of both *hsp90* isoforms revealed the existence of one out-of-frame downstream AUG codon at position +20 in *hsp90β*, which might be translated into a short polypeptide (17 amino acids). In addition, the nucleotide contexts (−7 to +4) of the downstream AUG contains two C at position −2 and a G at position +4, which would ordinarily confer an optimal context for translation than the initiator AUG codon (+1) (Fig. 2). The context of nucleotides flanking an AUG codon is known to be crucial for translation regulation [Kozak, 1986]. Accordingly, the better context an alternative downstream AUG is recognized, the greater inhibition of the normal open reading frame (ORF) may occur [Kozak, 1999]. Therefore, in our case scanning ribosomes might bypass the initiator AUG codon of *hsp90β*, and initiated translation at the second AUG codon with a better ribosome-binding context, just like the example of mouse *RX/rax* homeobox gene [Tucker et al., 2001]. To clarify the hypothesis in vitro, full-length *hsp90α* and *hsp90β* containing 5′- and 3′-UTR were cloned into pET21(+) vector, and two mutant constructs were also generated for IVTT assays (Fig. 3A). The protein expression of pET-*hsp90α* was 4.3-fold higher than that of pET-*hsp90β*. While the downstream AUG codon of *hsp90β* was mutated to AAG, pET-*hsp90β*m1, resulted in approximately 3.3-fold recovery of translation efficiency as compared to pET-*hsp90β* (Fig. 3B), suggesting that the downstream AUG of *hsp90β* may have a suppressive effect in translation efficiency.

Furthermore, when the mutant pET-*hsp90β*m2 construct containing the sequence CGCC**A**CCATG**G**, known as the Kozak context, was tested, the protein expression level of *hsp90β*m2 was significantly increased up to 3.5-fold when compared to that of

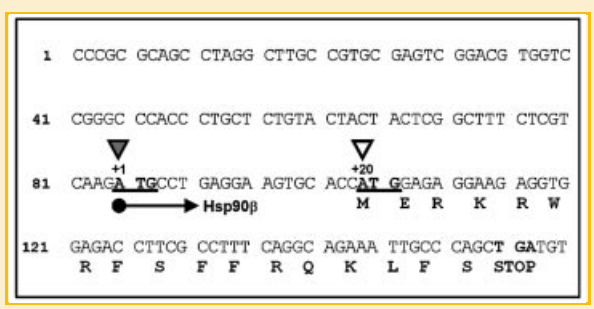

Fig. 2. The nucleotide sequence of the 5′-flanking region of the *hsp90β* from the transcription initiation site to the start codon. The AUG codon was underlined. The filled and open arrowheads indicate the positions of a translation initiation site in its own suboptimal Kozak context or in a perfect Kozak context, respectively. The arrows below the sequence was marked to present the translation in the initiator start site (+1) of natural Hsp90β protein or in the downstream AUG codon (+20) of a short peptide (17 amino acids). The deduced amino acid sequence of the downstream ORF is shown in the one-letter code.

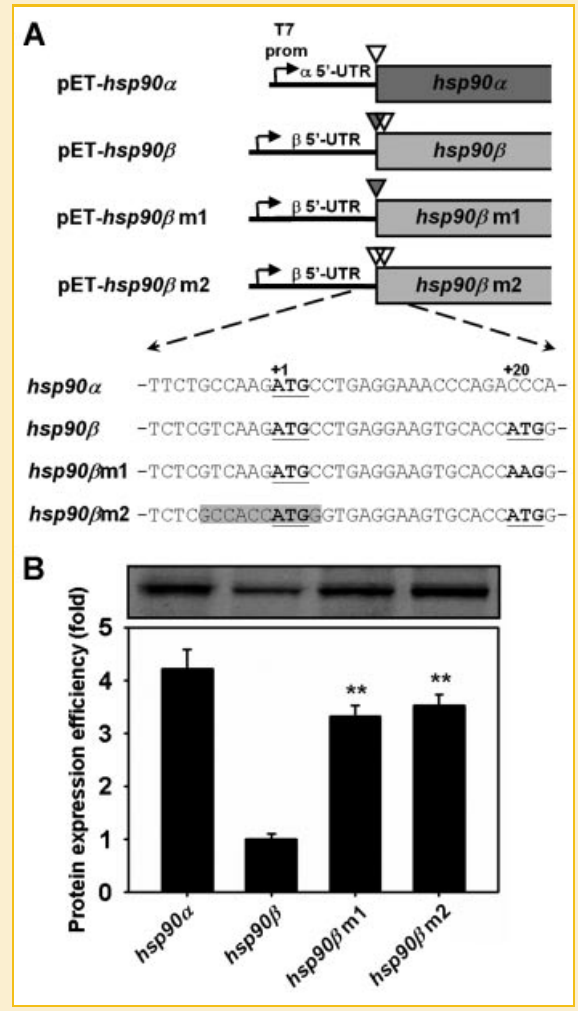

Fig. 3. Effect of leaky scanning mechanism on the translation efficiency of *hsp90β*. A: Schematic diagram of constructs for in vitro transcription and translation (IVTT) assay. The complete cDNA sequence of rat *hsp90α* and *hsp90β* with 5′- and 3′-UTR were cloned into pET21(+) vector to generate pET-*hsp90α* and pET-*hsp90β*, respectively. Sequence of hsp90β mRNA revealed the existence of one out-of-frame AUG codon (+20). The pET-*hsp90β*m1 was obtained by site-directed mutagenesis to generate point mutation (the second ATG → AAG), which abolished the translation ability of second start codon. The pET-*hsp90β*m2 was obtained by replacement of the initiator AUG context to Kozak context. The replacement sequence was indicated as gray region. The filled and open arrowheads indicate the positions of a translation initiation site in its own suboptimal Kozak context or in a perfect Kozak context, respectively. The start codon was underlined. B: Analysis of the translation efficiency by IVTT assay. SDS–PAGE analysis of [^{35}S]methionine-labeled proteins synthesized in a reticulocyte lysate programmed with equal amounts (1 μg) of each plasmids. The data represent means ± SD of three independent experiments; $^{**}P < 0.01$.

hsp90β, indicating that a stronger initiator AUG context could recruit ribosome complex more efficiently to initiate translation at the +1 position (Fig. 3B). Taken together, these in vitro translation results suggest that the original weak context of rat *hsp90β* initiator AUG has a lower potential for ribosome binding and consequently initiates translation on the downstream AUG codon by leaky scanning mechanism, which results in the reduction of the Hsp90β translation efficiency as showed in Figure 1.

TRANSLATION INITIATION ON THE DOWNSTREAM AUG CODON OF *hsp90β*

While translation initiation took place on the downstream AUG, the translational product of 17 amino-acid polypeptide should be expressed. However, it was too short to be detected. Therefore, the initiation of peptide synthesis employing firefly luciferase reporter assay was carried out. In the following reporter assay experiments, the 3′-UTR sequences downstream of the reporter coding sequence allowing high-level expression of firefly luciferase, SV40 late poly(A) signal and SV40 enhancer, were excised to exclude possible influence.

In the pGL3p/*hsp90β*, the *hsp90β* 5′- and 3′-UTR sequences were inserted upstream and downstream of the firefly luciferase, respectively (Fig. 4A). In addition, a pGL3p/*hsp90β** vector containing an insertion of *hsp90β* 5′-UTR element (5′-UTR*) from 5′ end to the +19 position upstream to the firefly luciferase was generated to mimic the upstream region of *hsp90β*. Instead of short polypeptide product, firefly luciferase should be expressed if ribosome initiated translation at the downstream AUG codon of *hsp90β*. The negative control, pGL3b showed no firefly luciferase activity, as expected (Fig. 4B, upper panel). The luciferase activity was observed in 9L cells transfected with the pGL3p/*hsp90β** construct, indicating successful initiation and translation of the downstream ORF. To confirm that the effect observed was not tissue specific, another human lung cancer cell line A549 was transfected with the same construct sets, and similar results were obtained (Fig. 4B, lower panel). These results suggest that ribosome scanning may bypass the first AUG and initiate at the next downstream AUG of *hsp90β*, thus resulting in premature translation termination and suppressive regulation.

REGULATION OF *hsp90* ISOFORMS TRANSLATION BY 5′-UTR SEQUENCE

To clarify the hypothesis whether the 5′-UTR sequence composition might have effects in translation efficiency, the 5′-UTR of *hsp90α* and *hsp90β* were swapped to generate pET-*βhsp90α* and pET-*αhsp90β* for IVTT assays (Fig. 5A). As compared with wild-type *hsp90α*, the chimera *βhsp90α* showed a slightly diminished translation efficiency (Fig. 5B). In contrast, the translation efficiency was elevated approximately twofold when *αhsp90β* was tested, suggesting that the 5′-UTR of *hsp90β* would lead to more reductive effect in translation efficiency. Moreover, the secondary structure, prediction carried out by RNA folding MFOLD software [Mathews et al., 1999] revealed that *hsp90β* 5′-UTR could form extensive and stable structure through approximately 90% base-pairing (Fig. 6A). To determine whether the stable structure of rat

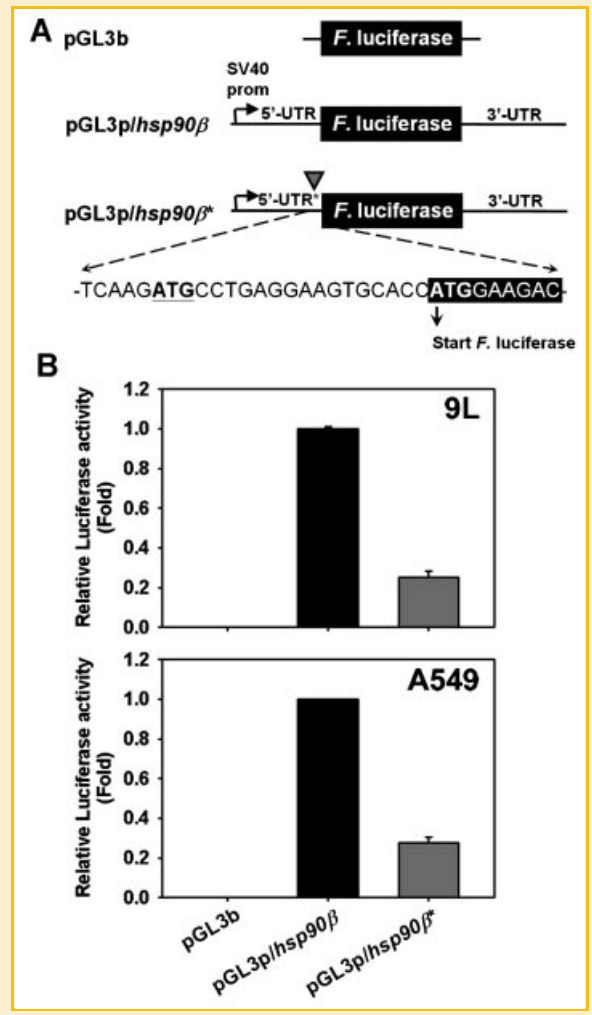

Fig. 4. Translation initiation on the downstream AUG codon of *hsp90β*. A: Schematic diagram of the pGL3b vector and different hsp90β 5′-UTR constructs in pGL3p vector. The pGL3p/*hsp90β* construct were generated by insertion of *hsp90β* 5′- and 3′-UTR sequence upstream and downstream of the firefly luciferase, respectively. The pGL3p/*hsp90β** was inserted the derived *hsp90β* 5′-UTR element (5′-UTR*) from 5′ end to the +19 position upstream the firefly luciferase. The filled arrowhead indicates the position of the translation initiation site of *hsp90β*. The start codon was underlined. The translation of firefly luciferase was indicated as black region of sequence. B: Constructs were co-transfected with pRL-CMV into 9L and A549 cells. The cells were harvested at 48 h after transfection. Firefly luciferase activities were normalized to *Renilla* luciferase activities. The relative luciferase activity values of pGL3b and pGL3p/*hsp90β** constructs were normalized to that of pGL3p/*hsp90β* construct. The data represent means ± SD of three independent experiments.

hsp90β 5′-UTR affected the translational efficiency, luciferase reporter constructs with truncated *hsp90β* 5′-UTR (pGL3p/*hsp90β*d1 and pGL3p/*hsp90β*d2) were designed (Fig. 6B,C) and their effects on translation were evaluated. As expected, truncated *hsp90β* 5′-UTR constructs showed a higher luciferase activity than that of pGL3p/*hsp90β*, strongly indicating that elimination of the secondary structure region in the 5′-UTR facilitated translation of *hsp90β* mRNA.

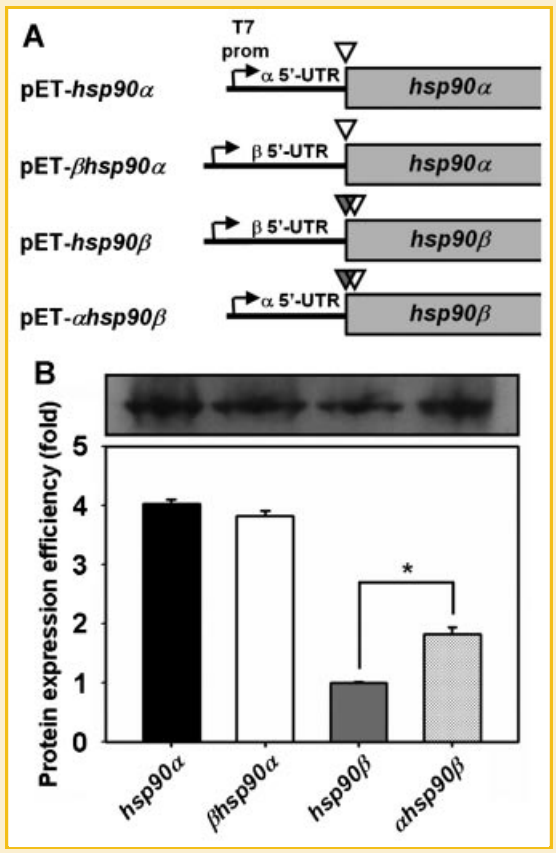

Fig. 5. Effect of 5′-UTR sequence on the translation efficiency of Hsp90 isoforms. A: Schematic diagram of constructs for IVTT assay. The pET-β*hsp90*α and pET-α*hsp90*β were generated by swapping 5′-UTR with each other. The filled and open arrowheads indicate the positions of a translation initiation site in its own suboptimal or optimal Kozak context, respectively. B: Analysis of the translation efficiency by IVTT assay. 10 percent SDS–PAGE analysis of [^{35}S]methionine-labeled proteins synthesized in a reticulocyte lysate programmed with equal amounts (1 μg) of each plasmids. The data represent means $\pm$ SD of three independent experiments; $^{*}P < 0.05$.

To ensure that the increase in firefly luciferase activity was correlated with the increase of translation, total RNA was isolated from transfected cells in parallel and subjected to RT-PCR and real-time qPCR analyses using specific firefly and *Renilla*

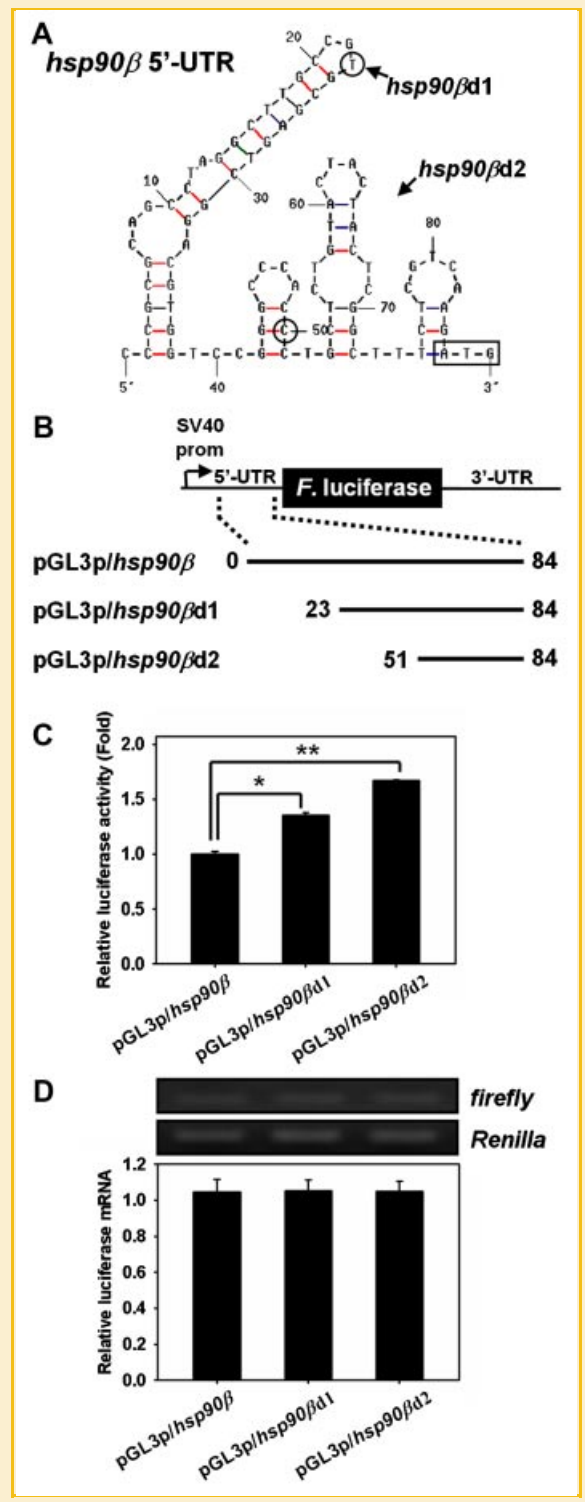

Fig. 6. Effects of *hsp90*β 5′-UTR sequence on the expression of firefly luciferase. A: The predicted structures of 5′-UTR sequence containing initiator AUG of *hsp90*β (87 bp) mRNA were fold by MFOLD program. The initiator AUG were indicated as the square region. The circled nucleotides represent the sites where 5′-UTR elements truncated to. B: Schematic diagram of constructs for luciferase reporter assay. The constructs were generated by insertion of *hsp90*β 5′-UTR and its truncated region into upstream the firefly luciferase of the pGL3p vector. C: Constructs were co-transfected with pRL-CMV into 9L cells. The cells were harvested at 48 h after transfection. Firefly luciferase activities were normalized to *Renilla* luciferase activities. The relative luciferase activities were calculated by the values of firefly luciferase of truncated *hsp90*β 5′-UTR constructs normalized and compared to that of *hsp90*β 5′-UTR constructs. The data represent means $\pm$ SD of at least three independent experiments; $^{*}P < 0.05$, $^{**}P < 0.01$. D: Total RNA of cells co-transfected with constructs and pRL-CMV were isolated from parallel transfected cells and subjected to RT-PCR and real-time qPCR as described in Materials and Methods Section. The relative mRNA amount of firefly luciferase was normalized by that of *Renilla* luciferase. Relative fold induction was calculated using the $\Delta\Delta C_t$ method. The data represent means $\pm$ SD of at least three independent experiments.

luciferase primer sets (Fig. 6D). The results showed that the increase in firefly luciferase activity in truncated 5′-UTR of *hsp90* mRNAs was not owing to changes in mRNA stability or transfection efficiency. Therefore, these findings suggest that *hsp90β* 5′-UTR forms stable RNA stem–loop structures and acts as a suppressive regulator for Hsp90β synthesis.

DISCUSSION

Our current studies have shown that differential expression of rat Hsp90 isoforms involves not only transcriptional control generally mediated by transcription factors [Chao et al., 2008], but also post-transcriptional control by differences in translation efficiency instead of the consequence of distinct mRNA or protein stability [Chang et al., 2006]. Herein, we have demonstrated that leaky scanning mechanism and the *hsp90β* 5′-UTR play important roles in negative regulation for *hsp90β* mRNA synthesis, which in turn result in a lower translational efficiency than that of *hsp90α* mRNA.

In terms of post-transcriptional level, previous studies have clearly indicated that the 5′-UTR of eukaryotic mRNA is a key factor for regulating gene expression. It is believed that most eukaryotic translation proceeds the ribosome-scanning model [Kozak, 1991a; Pestova and Kolupaeva, 2002], and undergoes predominantly a cap-binding mechanism [Kozak, 1999]. However, close proximity of the AUG codon to the 5′-end, presence of at least one AUG codon (upstream AUG) of the upstream ORF (uORF), binding of regulatory factors to mRNA, or extensive secondary structure preceding the initiator AUG would reduce the efficiency of translation at an AUG codon [McCarthy, 1998; Morris and Geballe, 2000]. Additionally, while a ribosome bypassing the first AUG codon, a short ORF translated in the downstream AUG codon may function like the conventional uORFs to affect RNA stability [Welch and Jacobson, 1999] or to produce a peptide [Bullock and Eisenlohr, 1996]. At the same time, the translation initiation in downstream AUG codon may retard the precise translation efficiency. Here, we have adopted two strategies to search for the potential regulatory mechanisms of rat *hsp90β* via this kind of conventional uORF effect.

First, in IVTT assay, we used point mutation at downstream AUG (ATG → AAG) to terminate the ribosome scanthrough effect in *hsp90β* and observed the increase in the translation efficiency (Fig. 3B). Furthermore, the introduction of Kozak context to the initiator AUG of *hsp90β* also increased the translation efficiency (Fig. 3B), suggesting that the negative effect might arise from context-dependent leaky scanning. Second, the insertion of sequence proceeding from the 5′ end to the downstream AUG of *hsp90β* in luciferase reporter assay allowed us to further demonstrate the leaky scanning effect (Fig. 4B). It should be noted that ribosome re-initiation is not responsible for the expression of *hsp90β*. Re-initiation mechanism should satisfy the condition when the first AUG codon initiates a small ORF that terminates before the start of the main ORF, and the main ORF can be then translated [Kozak, 2002a].

While the first and second AUG codons share the same reading frame, leaky scanning generates two proteins different in lengths, which sometimes have distinguishable functions. However, when the first and second AUG codons are in different reading frames, two completely unrelated proteins would be translated from one mRNA. The resulting uAUG-encoded products have been investigated in many viral and cellular mRNAs [Kozak, 1991a] that have widespread functions in biology. Most eukaryotic uORFs may either repress translation of the downstream ORF [Spotts et al., 1997; Mize et al., 1998], or affect on RNA stability [Ruiz-Echevarria and Peltz, 1996]. In this study, the downstream AUG of rat *hsp90β* may encode a 17 amino-acid polypeptide and then encounter the stop codon. The function of this short polypeptide, however, remains to be determined whether it is important for translational control or for other functions.

The 5′-UTR sequence of mRNA is also a well-studied factor for regulation of translation. For example, deletion of the Drosophila *hsp70* or *hsp22* 5′-UTR blocks translation during heat shock, whereas the cap-proximal 30 nucleotides partially preserve it [Lindquist and Petersen, 1990]. In this study, 5′-UTR swapping experiment performed in IVTT systems has shown that *hsp90β* 5′-UTR significantly exhibits the translation efficiency (Fig. 5B). Furthermore, the truncated 5′-UTR sequence results in an increase of firefly luciferase activity (Fig. 6B), indicating the presence of secondary structure may cause more reductive effect on translation efficiency of *hsp90β*. However, the highly folded 5′-UTR secondary structure might behave as cap-independent internal ribosome entry site (IRES). The translation efficiency via IRES-mediated mechanisms found in some viruses [Jackson, 1988; Lourenco et al., 2008] and eukaryotic mRNAs [Hellen and Sarnow, 2001; Vazquez-Padron et al., 2008] has been known, as the 5′-UTR sequences contain GC-rich and complex secondary structures. Except for the likely heat-activated IRES of that of *Drosophila* Hsp90 [Ahmed and Duncan, 2004], no IRES structure has so far been described in the 5′-UTR sequences of rat Hsp90 isoforms. Our recent results indicated that neither *hsp90α* not *hsp90β* 5′-UTR acts as an IRES (data not shown).

In conclusion, our data have demonstrated that rat Hsp90β expression is inhibited at the translational level via a leaky scanning mechanism. The 5′-UTR sequence is also involved in the inhibition of *hsp90β* translation, and the leaky scanning mechanism may be the dominantly repressive effect of translation efficiency. We provide several lines of evidence to reveal the major impact on the differential translation efficiency and regulation between *hsp90* isoforms.

REFERENCES

Ahmed R, Duncan RF. 2004. Translational regulation of Hsp90 mRNA. AUG-proximal 5′-untranslated region elements essential for preferential heat shock translation. J Biol Chem 279:49919–49930.

Bertram J, Palfner K, Hiddemann W, Kneba M. 1996. Increase of P-glycoprotein-mediated drug resistance by hsp 90 beta. Anticancer Drugs 7:838–845.

Bullock TN, Eisenlohr LC. 1996. Ribosomal scanning past the primary initiation codon as a mechanism for expression of CTL epitopes encoded in alternative reading frames. J Exp Med 184:1319–1329.

Chang YS, Lo CW, Sun FC, Chang MD, Lai YK. 2006. Differential expression of Hsp90 isoforms in geldanamycin-treated 9L cells. Biochem Biophys Res Commun 344:37–44.

Chao CC, Sun FC, Wang CH, Lo CW, Chang YS, Chang KC, Chang MD, Lai YK. 2008. Concerted actions of multiple transcription elements confer differential transactivation of HSP90 isoforms in geldanamycin-treated 9 L rat gliosarcoma cells. J Cell Biochem 104:1286–1296.

Chen B, Piel WH, Gui L, Bruford E, Monteiro A. 2005. The HSP90 family of genes in the human genome: Insights into their divergence and evolution. Genomics 86:627–637.

Csermely P, Schnaider T, Soti C, Prohaszka Z, Nardai G. 1998. The 90-kDa molecular chaperone family: Structure, function, and clinical applications. A comprehensive review. Pharmacol Ther 79:129–168.

Gress TM, Muller-Pillasch F, Weber C, Lerch MM, Friess H, Buchler M, Beger HG, Adler G. 1994. Differential expression of heat shock proteins in pancreatic carcinoma. Cancer Res 54:547–551.

Gupta RS. 1995. Phylogenetic analysis of the 90 kD heat shock family of protein sequences and an examination of the relationship among animals, plants, and fungi species. Mol Biol Evol 12:1063–1073.

Hansen LK, Houchins JP, O'Leary JJ. 1991. Differential regulation of HSC70, HSP70, HSP90 alpha, and HSP90 beta mRNA expression by mitogen activation and heat shock in human lymphocytes. Exp Cell Res 192:587–596.

Hellen CU, Sarnow P. 2001. Internal ribosome entry sites in eukaryotic mRNA molecules. Genes Dev 15:1593–1612.

Hickey E, Brandon SE, Smale G, Lloyd D, Weber LA. 1989. Sequence and regulation of a gene encoding a human 89-kilodalton heat shock protein. Mol Cell Biol 9:2615–2626.

Jackson RJ. 1988. RNA translation. Picornaviruses break the rules. Nature 334:292–293.

Jackson RJ. 2005. Alternative mechanisms of initiating translation of mammalian mRNAs. Biochem Soc Trans 33:1231–1241.

Jacquier-Sarlin MR, Jornot L, Polla BS. 1995. Differential expression and regulation of hsp70 and hsp90 by phorbol esters and heat shock. J Biol Chem 270:14094–14099.

Jameel A, Skilton RA, Campbell TA, Chander SK, Coombes RC, Luqmani YA. 1992. Clinical and biological significance of HSP89 alpha in human breast cancer. Int J Cancer 50:409–415.

Jerome V, Vourc'h C, Baulieu EE, Catelli MG. 1993. Cell cycle regulation of the chicken hsp90 alpha expression. Exp Cell Res 205:44–51.

Kozak M. 1986. Point mutations define a sequence flanking the AUG initiator codon that modulates translation by eukaryotic ribosomes. Cell 44:283–292.

Kozak M. 1989. Context effects and inefficient initiation at non-AUG codons in eucaryotic cell-free translation systems. Mol Cell Biol 9:5073–5080.

Kozak M. 1991a. An analysis of vertebrate mRNA sequences: Intimations of translational control. J Cell Biol 115:887–903.

Kozak M. 1991b. Structural features in eukaryotic mRNAs that modulate the initiation of translation. J Biol Chem 266:19867–19870.

Kozak M. 1999. Initiation of translation in prokaryotes and eukaryotes. Gene 234:187–208.

Kozak M. 2002a. Emerging links between initiation of translation and human diseases. Mamm Genome 13:401–410.

Kozak M. 2002b. Pushing the limits of the scanning mechanism for initiation of translation. Gene 299:1–34.

Kozak M. 2007. Some thoughts about translational regulation: Forward and backward glances. J Cell Biochem 102:280–290.

Laemmli UK. 1970. Cleavage of structural proteins during the assembly of the head of bacteriophage T4. Nature 227:680–685.

Lai MT, Huang KL, Chang WM, Lai YK. 2003. Geldanamycin induction of grp78 requires activation of reactive oxygen species via ER stress responsive elements in 9L rat brain tumour cells. Cell Signal 15:585–595.

Lee WC, Lee YC, Perng MD, Chen CM, Lai YK. 1993. Induction of vimentin modification and vimentin-HSP72 association by withangulatin A in 9L rat brain tumor cells. J Cell Biochem 52:253–265.

Lindquist S, Petersen R. 1990. Selective translation and degradation of heat-shock messenger RNAs in Drosophila. Enzyme 44:147–166.

Liu YV, Baek JH, Zhang H, Diez R, Cole RN, Semenza GL. 2007. RACK1 competes with HSP90 for binding to HIF-1alpha and is required for O(2)-independent and HSP90 inhibitor-induced degradation of HIF-1alpha. Mol Cell 25:207–217.

Livak KJ, Schmittgen TD. 2001. Analysis of relative gene expression data using real-time quantitative PCR and the 2(-Delta Delta C(T)) Method. Methods 25:402–408.

Lourenco S, Costa F, Debarges B, Andrieu T, Cahour A. 2008. Hepatitis C virus internal ribosome entry site-mediated translation is stimulated by cis-acting RNA elements and trans-acting viral factors. FEBS J 275: 4179–4197.

Mathews DH, Sabina J, Zuker M, Turner DH. 1999. Expanded sequence dependence of thermodynamic parameters improves prediction of RNA secondary structure. J Mol Biol 288:911–940.

McCarthy JE. 1998. Post-transcriptional control of gene expression in yeast. Microbiol Mol Biol Rev 62:1492–1553.

McCarthy JE, Kollmus H. 1995. Cytoplasmic mRNA-protein interactions in eukaryotic gene expression. Trends Biochem Sci 20:191–197.

Mize GJ, Ruan H, Low JJ, Morris DR. 1998. The inhibitory upstream open reading frame from mammalian S-adenosylmethionine decarboxylase mRNA has a strict sequence specificity in critical positions. J Biol Chem 273:32500–32505.

Moore SK, Kozak C, Robinson EA, Ullrich SJ, Appella E. 1989. Murine 86- and 84-kDa heat shock proteins, cDNA sequences, chromosome assignments, and evolutionary origins. J Biol Chem 264:5343–5351.

Morris DR, Geballe AP. 2000. Upstream open reading frames as regulators of mRNA translation. Mol Cell Biol 20:8635–8642.

Neckers L, Ivy SP. 2003. Heat shock protein 90. Curr Opin Oncol 15:419–424.

Ogata M, Naito Z, Tanaka S, Moriyama Y, Asano G. 2000. Overexpression and localization of heat shock proteins mRNA in pancreatic carcinoma. J Nippon Med Sch 67:177–185.

Pearl LH, Prodromou C. 2001. Structure, function, and mechanism of the Hsp90 molecular chaperone. Adv Protein Chem 59:157–186.

Pestova TV, Kolupaeva VG. 2002. The roles of individual eukaryotic translation initiation factors in ribosomal scanning and initiation codon selection. Genes Dev 16:2906–2922.

Picard D. 2002. Heat-shock protein 90, a chaperone for folding and regulation. Cell Mol Life Sci 59:1640–1648.

Pratt WB, Toft DO. 2003. Regulation of signaling protein function and trafficking by the hsp90/hsp70-based chaperone machinery. Exp Biol Med (Maywood) 228:111–133.

Racine T, Barry C, Roy K, Dawe SJ, Shmulevitz M, Duncan R. 2007. Leaky scanning and scanning-independent ribosome migration on the tricistronic S1 mRNA of avian reovirus. J Biol Chem 282:25613–25622.

Ruiz-Echevarria MJ, Peltz SW. 1996. Utilizing the GCN4 leader region to investigate the role of the sequence determinants in nonsense-mediated mRNA decay. EMBO J 15:2810–2819.

Shen Y, Liu J, Wang X, Cheng X, Wang Y, Wu N. 1997. Essential role of the first intron in the transcription of hsp90beta gene. FEBS Lett 413:92–98.

Shu CW, Cheng NL, Chang WM, Tseng TL, Lai YK. 2005. Transactivation of hsp70–1/2 in geldanamycin-treated human non-small cell lung cancer H460 cells: Involvement of intracellular calcium and protein kinase C. J Cell Biochem 94:1199–1209.

Spotts GD, Patel SV, Xiao Q, Hann SR. 1997. Identification of downstream-initiated c-Myc proteins which are dominant-negative inhibitors of transactivation by full-length c-Myc proteins. Mol Cell Biol 17:1459–1468.

Sreedhar AS, Mihaly K, Pato B, Schnaider T, Stetak A, Kis-Petik K, Fidy J, Simonics T, Maraz A, Csermely P. 2003. Hsp90 inhibition accelerates cell lysis. Anti-Hsp90 ribozyme reveals a complex mechanism of Hsp90

inhibitors involving both superoxide- and Hsp90-dependent events. J Biol Chem 278:35231–35240.

Sreedhar AS, Kalmar E, Csermely P, Shen YF. 2004. Hsp90 isoforms: Functions, expression and clinical importance. FEBS Lett 562:11–15.

Tucker P, Laemle L, Munson A, Kanekar S, Oliver ER, Brown N, Schlecht H, Vetter M, Glaser T. 2001. The eyeless mouse mutation (ey1) removes an alternative start codon from the Rx/rax homeobox gene. Genesis 31:43–53.

Vazquez-Padron RI, Pham SM, Mateu D, Khan S, Aitouche A. 2008. An internal ribosome entry site mediates the initiation of soluble guanylyl cyclase beta2 mRNA translation. FEBS J 275:3598–3607.

Wegele H, Muller L, Buchner J. 2004. Hsp70 and Hsp90—A relay team for protein folding. Rev Physiol Biochem Pharmacol 151:1–44.

Weizsaecker M, Deen DF, Rosenblum ML, Hoshino T, Gutin PH, Barker M. 1981. The 9L rat-brain tumor—Description and application of an animal-model. J Neurol 224:183–192.

Welch EM, Jacobson A. 1999. An internal open reading frame triggers nonsense-mediated decay of the yeast SPT10 mRNA. EMBO J 18:6134–6145.

Wu YP, Kita K, Suzuki N. 2002. Involvement of human heat shock protein 90 alpha in nicotine-induced apoptosis. Int J Cancer 100:37–42.

Yufu Y, Nishimura J, Nawata H. 1992. High constitutive expression of heat shock protein 90 alpha in human acute leukemia cells. Leuk Res 16:597–605.

Zhang SL, Yu J, Cheng XK, Ding L, Heng FY, Wu NH, Shen YF. 1999. Regulation of human hsp90alpha gene expression. FEBS Lett 444:130–135.